

Supporting information:

Chemoselective reduction of heteroarenes with a reduced graphene oxide supported rhodium nanoparticle catalyst

Alena Karakulina,^a Aswin Gopakumar,^a Zhaofu Fei^a and Paul J. Dyson^{a,*}

*a: Institut des Sciences et Ingénierie Chimiques, Ecole Polytechnique Fédérale de
Lausanne (EPFL), CH-1015, Lausanne, Switzerland.*

Contents

Figure S1. TEM micrographs of the rGO sheets.

Figure S2. Nitrogen adsorption-desorption isotherm of the rGO.

Figure S3. XPS survey spectrum of the rGO and the C1s spectrum.

Figure S4. TEM micrograph of Rh NP-rGO composite obtained by conventional thermal decomposition in [bmim][BF₄].

Figure S5. XRD pattern of the Rh NP-rGO composite obtained by microwave dielectric heating.

Figure S6. Comparison of ¹H NMR spectra of the ionic liquid [bmim][BF₄] before and after the catalysis.

Figure S7. Comparison of ¹³C NMR spectra of the ionic liquid [bmim][BF₄] before and after the catalysis.

Figure S8. Comparison of ¹⁹F NMR spectra of the ionic liquid [bmim][BF₄] before and after the catalysis.

Figure S9. ESI-MS of the reaction mixture before the catalysis.

Figure S10. ESI-MS of the reaction mixture after the catalysis.

Table S1. Hydrogenation of heteroarenes in water and glycerol using Rh NP-rGO catalyst.

References

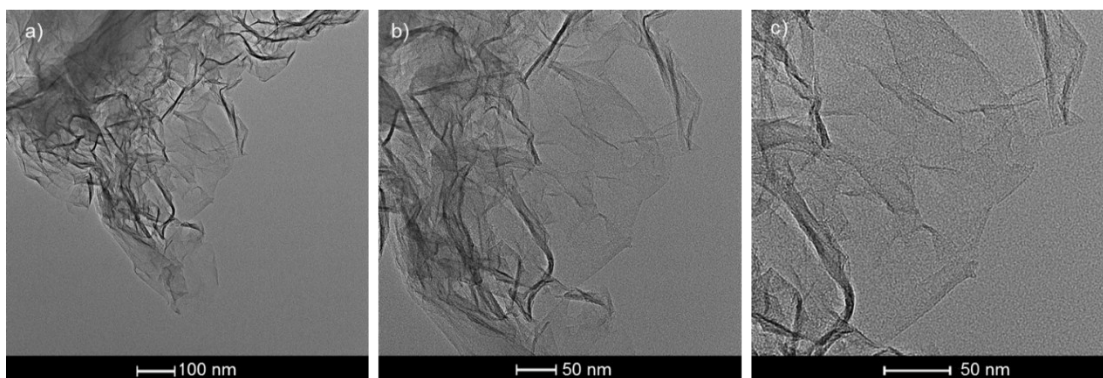


Figure S1. TEM micrograph of the rGO sheets (a) and the corresponding enlarged regions obtained at higher magnification (b) and (c).

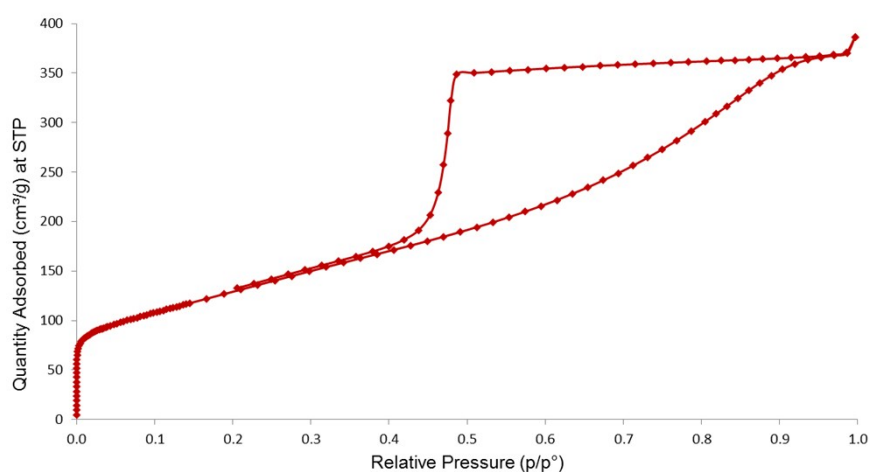


Figure S2. Nitrogen adsorption-desorption isotherm of the rGO. The formation of the hysteresis and the steep drop of the desorption branch at $P/P^0 \sim 0.5$ indicate the presence of small mesopores. This isotherm matches the reported isotherms of chemically reduced graphene oxide.¹ The reduced graphene oxide sample has the specific surface area of $470 \text{ m}^2/\text{g}$ (calculated using the BET equation). The high specific surface area can be used to evaluate the degree of exfoliation of the GO before its reduction. The theoretically estimated specific surface area of ideally exfoliated and isolated GO sheets is $2620 \text{ m}^2/\text{g}$,² indicating that agglomeration of the GO sheets occurred during the reduction process and resulted in the lower specific surface area. The agglomeration via overlapping and coalescing of the rGO sheets can lower the surface area of the bulk solid materials.¹ Nevertheless, the relatively high specific surface area of the obtained rGO indicates that the crumpled, wrinkled organization of the sheets provides a relatively large exposed surface.

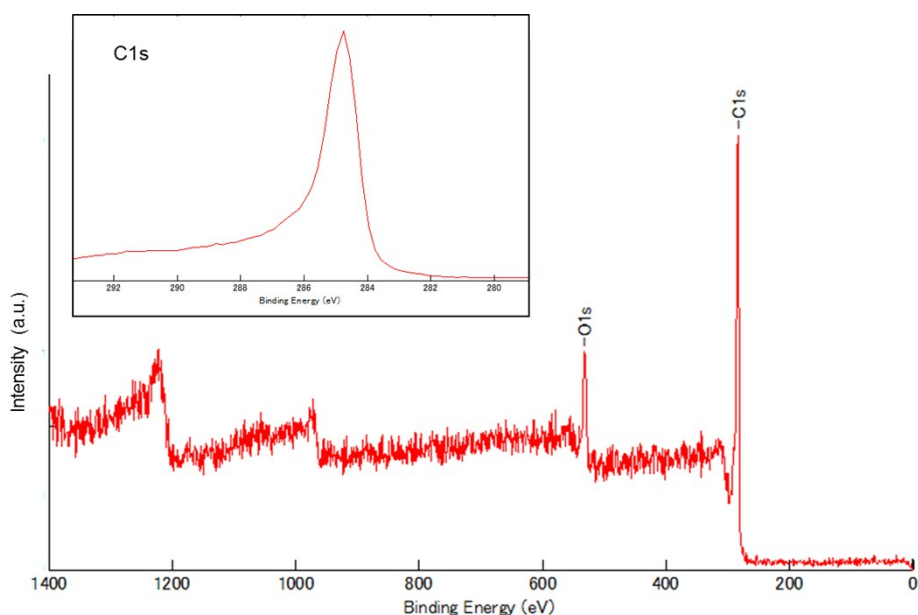


Figure S3. XPS survey spectrum of the rGO and the C1s spectrum (inset). The C1s XPS spectrum indicates the presence of a range of oxygen containing functionalities. Apart from the major peak at ca. 285 eV, a shoulder is observed at higher binding energies. The XPS spectra of GO and its reduced form typically display the presence of various species corresponding to carbon atoms in different functional groups, i.e. the non-oxygenated ring carbons (284.5 eV), carbons in C-O (286.5 eV), C=O (287.8 eV) and O=C-O (289.1 eV) bonds.³ The low peak intensities of these oxygen functionalities correspond to the residual broad shoulder in the XPS spectrum indicates that some functional groups have not been removed from the GO surface during the reduction process.^{1,4} Another peak at 285.9 eV attributed to the carbon bound to nitrogen was reported for the XPS spectrum of rGO obtained through hydrazine-assisted reduction method.^{1,5} It is usually difficult to remove all oxygen containing moieties from the GO surface and some functionalities are still present on the surface.^{4,6,7}

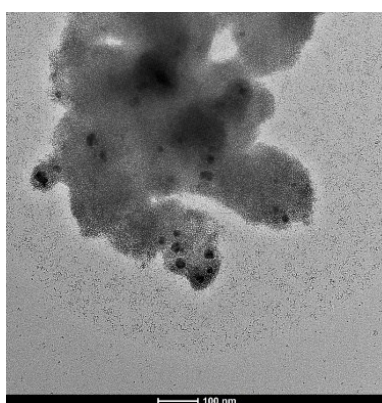


Figure S4. TEM micrograph of Rh NP-rGO composite obtained by conventional thermal decomposition in [bmim][BF₄].

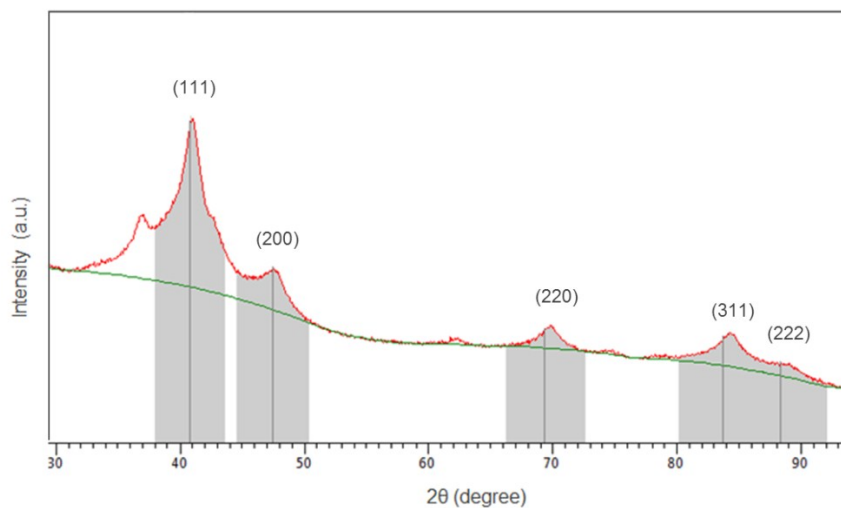


Figure S5. XRD pattern of the Rh NP-rGO composite obtained by microwave dielectric heating. Reference data for Rh was taken from the JCPDS card number 5-685. No diffraction peaks associated with a separated phase of rhodium oxide were detected, indicating that either the rhodium oxide phase is of low abundance, consistent with the XPS results, or as an amorphous oxide film, which is not observed by XRD.⁸ The shape of the diffraction lines indicates that the Rh NPs are nanocrystalline.

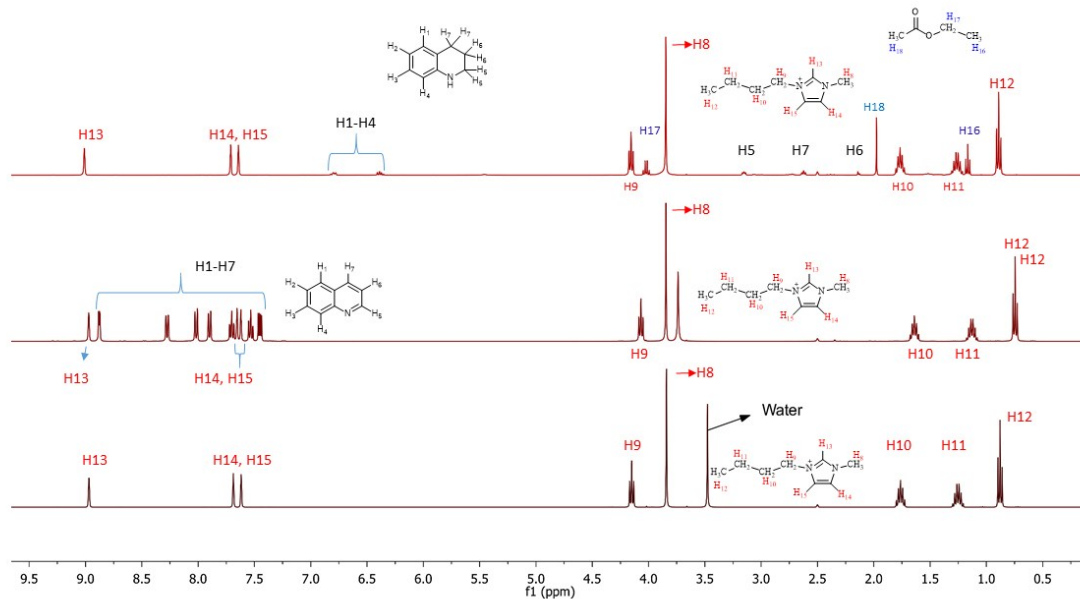


Figure S6. Comparison of ^1H NMR spectra of the ionic liquid [bmim][BF₄] before and after the catalysis in DMSO-*d*₆. Samples were filtered to remove the catalyst.

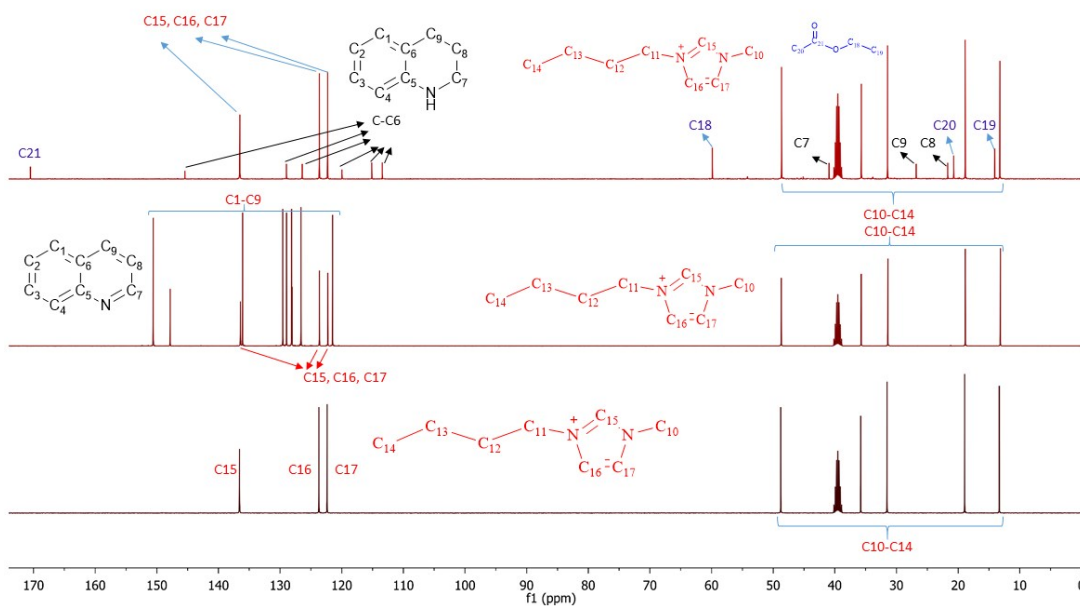


Figure S7. Comparison of ^{13}C NMR spectra of the ionic liquid [bmim][BF₄] before and after the catalysis in DMSO-*d*₆. Samples were filtered to remove the catalyst.

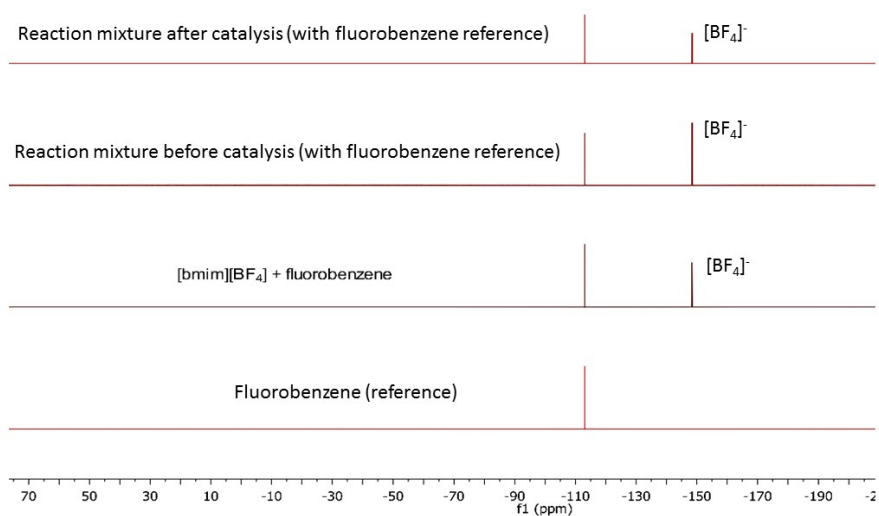


Figure S8. ^{19}F NMR spectra of fluorobenzene (reference), ionic liquid ($[\text{bmim}]\text{BF}_4$) and the reaction mixture before and after the catalysis in DMSO-d_6 (samples are filtered to remove the catalyst).

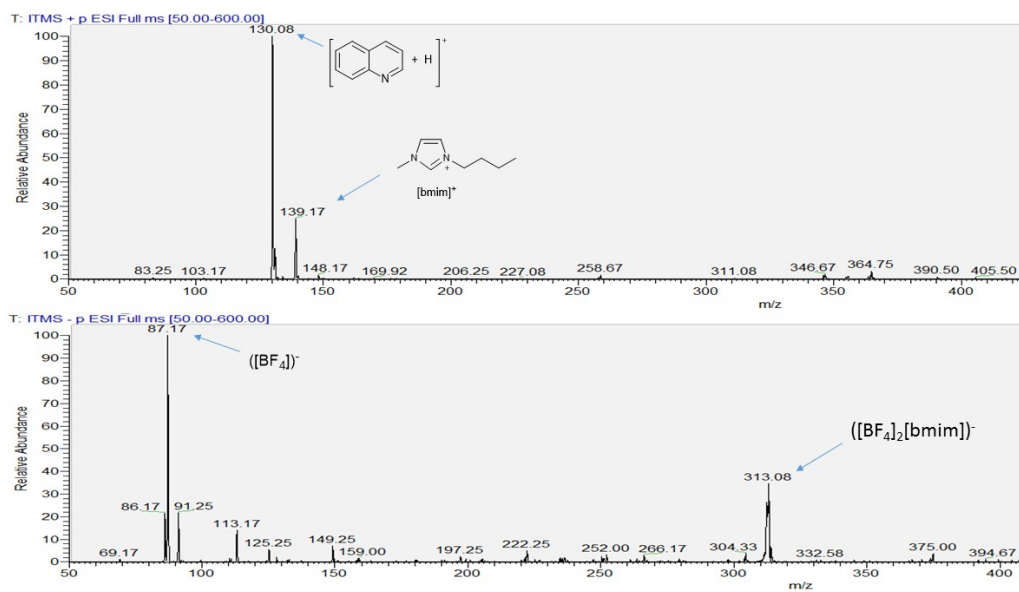


Figure S9. ESI-MS of the reaction mixture before the reaction; positive mode (top) and negative mode (bottom).

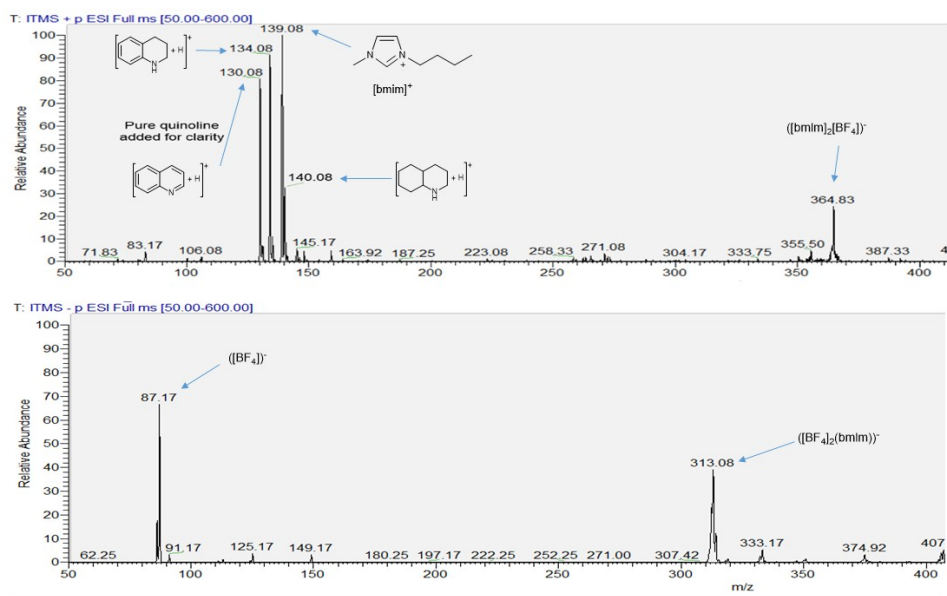
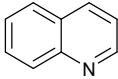
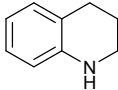
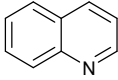
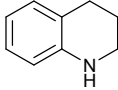
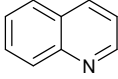
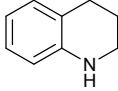
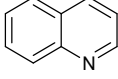
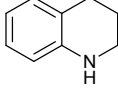
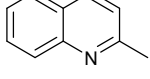
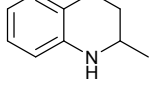
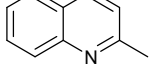
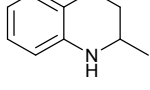
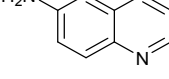
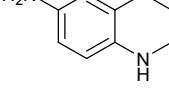


Figure S10. ESI-MS of the reaction mixture after the reaction; positive mode (top) and negative mode (bottom).

Table S1. Comparison of the hydrogenation of heteroarenes in water and glycerol using the Rh NP-

rGO catalyst.

Entry No.	Substrate	Time (h)	Solvent	Temperature (°C)	Yield[a] (%)	Product
1		10	Water	80	99	
2		10	Glycerol	80	99	
3		10	Water	50	99	
4		10	Glycerol	50	99	
5		10	Water	50	99	
6		10	Glycerol	50	99	
7		18	Water	80	90	
8		18	Glycerol	80	99	
9		15	Glycerol	80	90	

Reaction conditions: Rh NP-rGO catalyst (1 mol%), substrate (1 mmol), solvent (1 mL), H₂ (10 bar), Yield determined by GC.

References

1. S. Stankovich, D. A. Dikin, R. D. Piner, K. A. Kohlhaas, A. Kleinhammes, Y. Jia, Y. Wu, S. T. Nguyen and R. S. Ruoff, *Carbon*, 2007, **45**, 1558-1565.
2. S. Stankovich, D. A. Dikin, G. H. B. Dommett, K. M. Kohlhaas, E. J. Zimney, E. A. Stach, R. D. Piner, S. T. Nguyen and R. S. Ruoff, *Nature*, 2006, **442**, 282-286.
3. J. F. Moulder, *Handbook of X-ray Photoelectron Spectroscopy: A Reference Book of Standard Spectra for Identification and Interpretation of XPS Data*. Physical Electronics Division, Perkin-Elmer Corporation, 1992.

-
4. M. Tan, G. Yang, T. Wang, T. Vitidsant, J. Li, Q. Wei, P. Ai, M. Wu, J. Zheng and N. Tsubaki, *Catal. Sci. Technol.*, 2016, **6**, 1162-1172.
 5. H. Yang, C. Shan, F. Li, D. Han, Q. Zhang and L. Niu, *Chem. Commun.*, 2009, 3880-3882.
 6. S. Pei and H.-M. Cheng, *Carbon*, 2012, **50**, 3210-3228.
 7. C. Ma, Y. Du, J. Feng, X. Cao, J. Yang and D. Li, *J. Catal.*, 2014, **317**, 263-271.
 8. M. Choi, M. H. Seo, H. J. Kim and W. B. Kim, *Synth. Met.*, 2011, **161**, 2405-2411.